The effect of transformer Winding

by Hanny Tumbelaka

Submission date: 11-Dec-2020 03:37PM (UTC+0700)
Submission ID: 1471928549
File name: Binder.pdf (1.39M)
Word count: 7406
Character count: 40723

International Journal of Renewable Energy Research-IJRER

International Journal of Renewable Energy Research (IJRER)

The *International Journal of Renewable Energy Research* (IJRER) is not a for profit organisation. IJRER is a quarterly published, open source journal and operates an online submission with the peer review system allowing authors to submit articles online and track their progress via its web interface. IJRER seeks to promote and disseminate knowledge of the various topics and technologies of renewable (green) energy resources. The journal aims to present to the international community important results of work in the fields of renewable energy research, development, application or design. The journal also aims to help researchers, scientists, manufacturers, institutions, world agencies, societies, etc. to keep up with new developments in theory and applications and to provide alternative energy solutions to current issues such as the greenhouse effect, sustainable and clean energy issues.

The IJRER journal aims for a publication speed of 60 days from submission until final publication.

The coverage of IJRER includes the following areas, but not limited to:

- Green (Renewable) Energy Sources and Systems (GESSs) as Wind power,Hydropower, Solar Energy, Biomass, Biofuel, Geothermal Energy, Wave Energy, Tidal energy, Hydrogen & Fuel Cells, Li-ion Batteries, Capacitors
- New Trends and Technologies for GESSs
- Policies and strategies for GESSs
- Production of Energy Using Green Energy Sources
- Applications for GESSs
- Energy Transformation from Green Energy System to Grid
- Novel Energy Conversion Studies for GESSs
- Driving Circuits for Green Energy Systems
- Control Techniques for Green Energy Systems
- Grid Interactive Systems Used in Hybrid Green Energy Systems
- Performance Analysis of Renewable Energy Systems
- Hybrid GESSs
- Renewable Energy Research and Applications for Industries
- GESSs for Electrical Vehicles and Components
- Artificial Intelligence Studies in Renewable Energy Systems
- Computational Methods for GESSs
- Machine Learning for Renewable Energy Applications
- GESS Design
- Energy Savings
- Sustainable and Clean Energy Issues
- Public Awareness and Education for Renewable Energy

USER
Username
Password
Remember me
Login

NOTIFICATIONS
- View
- Subscribe

JOURNAL CONTENT
Search
Search Scope
All
Search

Browse
- By Issue
- By Author
- By Title

FONT SIZE

INFORMATION
- For Readers
- For Authors
- For Librarians

Journal Help

- Future Directions for GESSs
- Thermoelectric Energy

Online ISSN: 1309-0127

IJRER is cited in SCOPUS, EBSCO, WEB of SCIENCE (Clarivate Analytics);

WEB of SCIENCE;

h=9,

Average citation per item=1.84

Impact Factor=686/544=1.261

Announcements

icSmartGrid International Conference on Smart Grid

www.icSmartGrid.org

Posted: 2018-11-03

IJRER is in the Emerging Sources Citation Index on Web of S

IJRER has been cited in Emerging Sources Citation Index from 2015 in web of sc

h=9, Average citation per item=1.84

Impact Factor=686/544=1.261

Posted: 2018-03-19

IJRER Citation in SCOPUS-November-2018

2014 CiteScore	2014 SJR	2014 SNIP	2015 CiteScore	2015 SJR	2015 SNIP	2016 CiteScore	2016 SJR	20: SN
0.90	0.237	0.740	0.87	0.296	0.798	0.94	0.286	0.5

Posted: 2017-08-14

Impact Factor of IJRER

http://www.scimagojr.com/journalsearch.php?q=21100258747&tip=sid

SCOPUS SCIMAGO Journal Ranking

Rank	Sourceid	Issn	SJR	SJR Best Quartile	H index	Total Docs. (2017)	Tota Docs (3ye
14688	21100258747	13090127	0,262	Q3	18	227	461

---

http://www.doaj.org/doaj?func=findJournals&uiLanguage=en&hybrid=&query=i

International Journal of Renewable Energy Research-IJRER

Vol 8, No 1 (2018)

Vol8

Table of Contents

Articles

5
An Evaluation of Charging Power Balance of EV Battery for Household Distributed Power System — PDF — Invited Paper 1-6
Shinichiro Hattori, Haruhi Eto, Fujio Kurokawa, Kazuhiro Kajiwara

The Impact of Transformer Winding Connections of A Grid-Connected PV on Voltage Quality Improvement — PDF — 7-14
Hanny Tumbelaka, Eduard Muljadi, Wenzhong Gao

Wind Turbine Condition Monitoring using Multi-Sensor Data system — PDF — 15-25
Khalid Fatihi Abdulraheem, Ghassan Al-Kindi

3
Automatic Generation Contol Including Solar Themal Power Generation with Fuzzy-PID controller with Derivative Filter — PDF — 26-35
Manoj Kumar Debnath, Sayantan Sinha, Ranjan Kumar Mallick

Power Flow Control of PV-Wind-Battery Hybrid Renewable Energy Systems for Stand-Alone Application — PDF — 36-43
Somnath Das, Ashok Kumar Akella

Real Time Estimation of SOC and SOH of Batteries — PDF — 44-55
venkatesh prasad, B.P. divakar

Optimization of Size and Cost of Static VAR Compensator using Dragonfly Algorithm for Voltage Profile Improvement in Power Transmission Systems — PDF — 56-66
J Vanishree, V Ramesh

3
Study and Analysis of Performance of 3-Phase Shunt Active Filter in Grid-tied PV-Fuel Cell System Employing Sinusoidal Current Control Strategy — PDF — 67-81
RUDRANARAYAN SENAPATI

The Photocurrent and Spectral Response of a Proposed p+p n n+ Silicon Solar Cell — PDF — 82-89
Ashim Kumar Biswas, Sayantan Biswas, AMITABHA SINHA

Evaluation of Effects of Compression Ratio on Performance, Combustion, Emission, Noise and Vibration Characteristics of a VCR Diesel Engine — PDF — 90-100
Şafak Yıldızhan, Erinç ULUDAMAR, Mustafa ÖZCANLI, Hasan SERİN

Energy Resource Management Integrating Generation, Load Control and Change in Consumption Habits at the Residential — PDF — 101-107

Level
Adriana Marcela Vega, Dario Amaya, Francisco Santamaría, Edwin Rivas

An Efficient and Low-Cost Single-Stage PV Pumping System: Experimental Investigation Based on Standard Frequency Converter — PDF 108-119
Mansour MILADI, Afef BENNANI-BENABDELGHANI, Ilhem SLAMA BELKHODJA

Experimental Study on the Organic Rankine Cycle for Recovering Waste Thermal Energy — PDF 120-128
Soo-Yong cho, Chong-Hyun Cho, Yang-Beom Jung

Security-constrained Economic Dispatch with Linear/Nonlinear Energy Sources during Short-Term Emergency Period — PDF 129-140
Issam Smadi, Saher Albatran, Mohammad Alathamneh, Muwaffaq Alomoush

A State of Art Review on Offshore Wind Power Transmission Using Low Frequency AC System — PDF 141-149
Seetha Chaithanya, V Naga Bhaskar Reddy, R Kiranmayi

A Review: Control Strategies for Power Quality Improvement in Microgrid — PDF 150-165
Lavanya Viswanathan, SENTHIL KUMAR

Optimal sizing and placement of DG units in radial distribution system — PDF 166-177
sirine Essallah, Adel Bouallegue, Adel Khedher Khedher

Implementation of an improved Coulomb-Counting Algorithm Based on a Piecewise SOC-OCV Relationship for SOC Estimation of Li-Ion Battery — PDF 178-187
ines Baccouche, sabeur Jemmali, Asma Mlayah, Bilal Manai, Najoua Essoukri Ben Amara

Integrated Demand Side Management and Generation Control for Frequency Control of a Microgrid Using PSO and FA based Controller — PDF 188-199
Abdul Latif, Dulal Chandra Das, Sudhanshu Ranjan, Israfil Hussain

GA Based Optimization for Configuration and Operation of Emergency Generators in Medical Facility Using Renewable Energy — PDF 200-207
Masaharu Tanaka, Haruhi Eto, Yuji Mizuno, Nobumasa Matsui, Fujio Kurokawa

Performance Analysis of Grid connected PV/Wind Hybrid Power System during Variations of Environmental Conditions and Load — PDF 208-220
Ahmed Mohammed Ahmed Ibrahim, Omar Noureldeen

Enhanced Hybrid Global MPPT Algorithm for PV Systems operating under Fast-Changing Partial Shading Conditions — PDF 221-229
Santi Agatino Rizzo

Comparative Study on Module Connections to Minimize Degradation of Photovoltaic Systems due to Bird Droppings — PDF 230-237
Chaeyoung Lee, Jangwon Suh, Yosoon Choi

Optimal Planning of a Multi-Carrier Microgrid (MCMG) Considering Demand-Side Management — PDF 238-249
Vahid Amir, Shahram Jadid, Mahdi Ehsan

Assessment of the performance for a new design of storage solar collector — PDF 250-257
omer khalil

Design and Construction of a Stand-Alone PV System for Charging Mobile Devices in Urban Landscapes in Medellin — PDF 258-265
Eduardo Alexander Duque Grisales, Juan David Gonzalez Ruiz, Paola Maritza Ortíz Grisales, Anderson Felipe Lujan Tobón, Sebastián Chica Lopez, Andrés Felipe Isaza Piedrahíta

An improved control strategy using RSC of the wind turbine based on DFIG for grid harmonic currents mitigation — PDF 266-273
Moussa REDDAK

Viability study of implementing cross flow helical turbine for Micropower generation in India — PDF 274-279
V. jayaram

PV System Analysis Under Partial Shading Using a Sine Model — PDF 280-290
L Navinkumar Rao, Sanjay Gairola

Numerical Simulation of Flow through Invelox Wind Turbine System — PDF 291-301
Snehal Narendrabhai Patel

Assessment of the Environmental Impact of Biomass Electricity Generation in Thailand — PDF 302-312
Wasin Khaenson, Somchai Maneewan, Chantana Punlek

An Aqua Based Reduced Graphene Oxide Nanofluids for Heat Transfer Applications: Synthesis, Characterization, Stability Analysis, and Thermophysical Properties — PDF 313-319
KAMATCHI R, Gopi Kannan K

Energy Control Strategy for Large-Scale Grid Connected PV System with Batteries — PDF 320-327
abdulkadir hamid

Power Flow Control in Virtual Power Plant LV Network — PDF 328-335
Elena Sosnina, Alexandr Chivenkov, Andrey Shalukho, Nikita Shumskii

Dynamic Reconfiguration of Electrical Connections for partially shaded PV Modules: Technical and Economical Performances of an Arduino-based Prototype — PDF 336-344
Massimo Caruso, Patrizia Livreri, Giuseppe Schettino, Vincenzo Castiglia, Filippo Pellitteri

Simultaneous Distribution Network Reconfiguration and Optimal Distributed Generations Integration using a Pareto Evolutionary Algorithm — PDF 345-356
Imen BEN HAMIDA, Saoussen Brini Salah, Faouzi Msahli, Mouhamed Faouzi Mimouni

Design the Optimal Number of Components in a Grid-Connected Hybrid Power Generation System — PDF 357-364
mahdi heidari

Experimental Investigation of Temperature Effect on PV Monocrystalline Module — PDF 365-373
Heba Ahmed Mosalam

Performance Analysis of Grid-Connected Wind Turbine System Under Inter-Turn-Short-Circuit Fault Conditions — PDF 374-383
takwa sellami, hanen berriri, sana jelassi, abdel moumen darcherif, med faouzi mimouni

Backstepping Control of Dual Stator Induction Generator used in Wind Energy Conversion System — PDF 384-395
MERYEM BENAKCHA

Overcurrent Protection Assessment with high PV Penetration in a Distribution Network — PDF 396-406
Yeboh Ngalo Lucky de Marco, Tao Zheng, Srete N. Nikolovski

Light liquid fuel from catalytic cracking of beef tallow with ZSM-5 — PDF 407-413
Thapanapong Khammasan, Nakorn Tippayawong

The Silica-Alumina Based Catalytic Cracking of Bio-oil Using Double Series Reactor — PDF 414-420
sunarno sunarno, Arief Budiman, Rochmadi Rochmadi, Panut Mulyono

Effect of Temperature on Catalytic Decomposition of Tar using Indonesian Iron Ore as Catalyst — PDF 421-427
Doni Rahmat Wicakso, Sutijan Sutijan, Rochmadi Rochmadi, Muslikhin Hidayat, Rochim Bakti Cahyono, Arief Budiman

Modified Second Order Adaptive Filter for Grid Synchronization and Reference Signal Generation — PDF 428-437
Banishree Misra, Byamakesh Nayak

Comparative Studies of Cell Growth, Total Lipid and Methyl Palmitate of Ankistrodesmus sp. In Phototrophic, Mixotrophic and Heterotrophic Cultures For Biodiesel Production — PDF 438-450
Rachel Fran Mansa, Coswald Stephen Sipaut, Suhaimi Md. Yasir, Jedol Dayou, Costantine Joannes

Optimum Extraction of Algae-oil from Microalgae using Hydrodynamic Cavitation — PDF 451-458

Martomo Setyawan, Arief Budiman, Panut Mulyono, - Sutijan

Evaluation of energy yield ratio (EYR), energy payback period (EPBP) and GHG-emission mitigation of solar home lighting PV-systems of 37Wp modules in India — PDF 459-465
BHUPENDRA SINGH RAWAT, Poonam Negi, P. C. Pant, G. C. Joshi

Optimization of Acid Hydrolysis Process on Macro-alga Ulva lactuca for Reducing Sugar Production as Feedstock of Bioethanol — PDF 466-475
Tri Poespowati

A DWT Based Differential Relaying STATCOM Integrated Wind Fed Transmission Line — PDF 476-487
Sanjay Kumar Mishra, Loknath Tripathy, Sarat Chandra Swain

Cost minimization strategy for satellite solar power station — PDF 488-494
DEEPAK KUMAR, kalpana chaudhary

An Extended Model to Analyze Energy Saving: Parameters and Composition — PDF 495-503
Kamal JEMMAD, Abdelhamid HMIDAT, Abdallah SAAD

Simulation and Comparison of Helical and Straight-bladed Hydrokinetic Turbines — PDF 504-513
Mehmet Ishak YUCE, Mohammad A. Al-DABBAGH

FDTD based Plasmonic Light Trapping Analysis in Thin Film Hydrogenated Amorphous Silicon Solar Cells — PDF 514-522
Chetan V Radder

Economic Analysis of Integrated Renewable Energy System for Electrification of Remote Rural Area Having Scattered Population — PDF 523-539
Alpeshkumar Mangaldas Patel, Sunil Kumar Singal

CFD Based Optimization of Oscillatory Wing Motion for Maximum Energy Harvesting from Wind — PDF 540-551
Mustafa Kaya, Munir Ali Elfarra

MATLAB Simscape Model of An Alkaline Electrolyser and Its Simulation with A Directly Coupled PV Module for Auckland Solar Irradiance Profile — PDF 552-560
David Martinez, Ramon Zamora

Multi agent system design for PV integrated home management — PDF 561-574
mariam elloumi

Evaluation of The Wind Energy Potential of Thailand considering its Environmental and Social Impacts using Geographic Information Systems — PDF 575-584
Chanokporn Smuthkalin, Takehiko Murayama, Shigeo Nishikizawa

Implementation and Performance Analysis of a Single Phase Synchronization Technique based on T/4 Delay PLL — PDF 585-591
iwan setiawan, Trias Andromeda, Mochammad Facta, Hermawan Hermawan, Susatyo Handoko

Analysis of Power Quality Factor of Hybrid Energy System Supplying Three Phase Load — PDF 592-603
S. K. Bhuyan, Prakash Kumar Hota, B. Panda

A Simple Synchronization Logic Aided Interleaved Fly-Back MIC for Grid Interactive Photovoltaic Power System — PDF 604-613
SOMASHREE PATHY, SUBRAMANI C, SRIDHAR R, DASH S S

Geothermal Energy Potential of Arjuno and Welirang Volcanoes Area, East Java, Indonesia — PDF 614-624
Untung Sumotarto

Comparative Analysis of Designing Solar and Geothermal Power Plants: A Case Study — PDF 625-634
Roberto Venegas, Sarada Kuravi, Krishna Kota, Mary McCay

What are the Current Status and Future Prospects in Solar Irradiance and Solar Power Forecasting? — PDF 635-648
Mehmet Yesilbudak, Medine Colak, Ramazan Bayindir

Global Solar Radiation of some Regions of Cameroon using the Linear Angstrom Model and Non-linear Polynomial Relations: Part 2, Sun-path Diagrams, Energy Potential Predictions and Statistical Validation — PDF 649-660

Afungchui David, Ebobenow Joseph, Neba Rene Ngwa,
Nkongho Ayuketang Arreyndip

Online ISSN: 1309-0127

www.ijrer.org

ijrereditor@gmail.com; ilhcol@gmail.com;

IJRER is cited in SCOPUS, EBSCO, WEB of SCIENCE (Clarivate Analytics)

WEB of SCIENCE;

h=9,

Average citation per item=1.84

Impact Factor=686/544=1.261

The Impact of Transformer Winding Connections of a Grid-Connected PV on Voltage Quality Improvement

Hanny H. Tumbelaka*‡, Eduard Muljadi**, Wenzhong Gao***

*Department of Electrical Engineering, Petra Christian University, Surabaya, Indonesia

**National Renewable Energy Laboratory (NREL), Golden, Colorado, USA

***Department of Electrical & Computer Engineering, University of Denver, Denver, Colorado, USA

(tumbeh@petra.ac.id, Eduard.Muljadi@nrel.gov, Wenzhong.Gao@du.edu)

‡Corresponding Author: Hanny H. Tumbelaka, Petra Christian University, Indonesia, Tel: +62 31 2983442, tumbeh@petra.ac.id

Received: 09.05.2017 Accepted:09.09.2017

Abstract- In this paper, a high-power PV power plant is connected to the weak grid by means of a three-phase power transformer. The selection of transformer winding connection is critical especially when the PV inverter has a reactive power controller. In general, transformer winding connection can be arranged in star-star (with neutrals grounded) or star-delta. The reactive power controller supports voltage regulation of the power system particularly under transient faults. Its control strategy is based on utilizing the grid currents to produce a three-phase unbalanced reactive current with a small gain. The gain is determined by the system impedance. Simulation results exhibit that the control strategy works very well particularly under disturbance conditions when the transformer winding connection is star-star with both neutrals grounded. The power quality in terms of the voltage quality is improved.

Keywords- Grid connected PV; Reactive power; Transformer winding; Voltage quality

1. Introduction

Nowadays, the utilization of renewable power sources has expanded extensively to replace petroleum product based energy sources. Wind, hydro and sunlight based energy sources are among those renewable power sources. Those energy sources are sustainable, ecologically benevolent and do not result in the climate change.

Renewable energy sources can be connected directly to loads (as a stand alone system) or to an electric power AC grid. These days, most of the renewable energy sources such as Photovoltaic (PV) panels are attached to the grid [1,2]. As the output of the PV panels is in DC voltage and current, it needs a DC-AC converter to deliver the power to the grid.

To connect the inverter to the grid, the DC bus voltage of the inverter must be higher than the peak value of the grid voltage [3]. To achieve the required DC bus voltage level, several PV arrays have to be arranged in series. The voltage rating of the devices must also be chosen to withstand the same level of voltage with enough voltage margin to survive during transient events.

A multilevel inverter could be one of solutions to the high voltage problem [4,5,16]. But, the multilevel inverter needs many switches and a complex controller. Another solution is to install a step-up transformer [1,2,6,7] between the PV inverter and the grid so that the PV inverter can work in a low voltage level. This solution is simple and easy to implement. Complex combination of multilevel inverters and a transformer [14,15] is possible for a special application.

In general, transformer primary and secondary windings are connected in star-star (with both neutrals grounded) or star-delta. The selection of transformer winding connection may affect the inverter controller. Because different winding connections may introduce a phase shift between the line

currents in the primary winding and in the secondary winding. The phase shift, if not considered, will give incorrect output than the commanded reference values. Hence, this paper will study the impact of transformer winding connection on the PV inverter operation especially under fault conditions.

The main contribution of this paper is to develop a new control strategy so that the PV inverter can support voltage regulation at the point of common coupling particularly under transient faults, which include both symmetrical and unsymmetrical faults. The control strategy is based on fault analysis and calculation of a grid current to compensate for a three-phase unbalanced reactive current. The paper first presents an average circuit model for PV generator along with the new reactive power control strategy. Typical transformer connection types for PV inverter application are described in details. Then a power system with PV distributed generation via weak connection is analyzed to reveal the compensation strategy for voltage quality improvement. Extensive simulation studies are presented to show the effectiveness of the new control strategy under different faults and different transformer connections.

2. PV Installation

2.1 PV Model

The PV generator consists of PV arrays and a grid-connected PV inverter. The DC bus of the PV inverter is connected to PV panels, and the AC output terminal is attached to the grid via a step-up transformer. PV arrays usually work as a current source controlled by the strength of solar irradiance. The PV inverter more often operates in a current-controlled mode. The current controller regulates the inverter output currents delivered to the grid. Assumed that the switching frequency of the inverter is very high, as such that the output currents of the three-phase inverter are purely sinusoidal. Hence, the average circuit model uses a three-phase dependent current source model to represent the PV arrays with the three phase PV inverter.

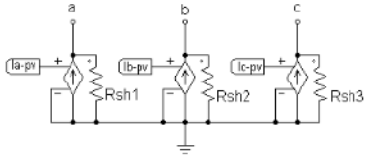

Fig. 1. A three-phase PV average model.

The PV inverter output current comprises of the active and reactive current. The measure of active power conveyed to the power system is dictated by the intensity of sunlight as well as the environment surrounding the PV panels. To get maximum active power, the PV inverter is upheld by a MPPT controller. The amount of reactive power flow is regulated by a reactive power controller of the PV inverter since the PV arrays just generate active power. The Norton equivalent circuit of the PV model is appeared in Figure 1, where $I_{a\text{-}pv}$, $I_{b\text{-}pv}$ and $I_{c\text{-}pv}$ are the reference or commanded currents of the PV inverter.

2.2 Reactive Power Control

Since power system demands reactive power for voltage regulation, the PV inverter is equipped with a reactive power controller. Subsequently, the PV inverter should be able to compensate for the voltage drop along the line impedance in normal and under fault conditions to a certain extent, with the purpose to regulate the grid voltage. Thus, it reduces network losses and increases transmission limit.

Many literatures can be found about reactive power control for a grid-connected PV inverter [7-11,17]. A PV inverter generally can be controlled to draw or to supply reactive power depending upon inverter control strategies chosen (e.g constant voltage, constant reactive power, and constant power factor). The control strategy could employ a PI controller or a V-Q slope characteristic as well as an intelligent controller [12]. Moreover, the amount of reactive power provided by the PV inverter could likewise be resolved from the active power flow related to system impedance R/X ratio.

In this paper, a new control strategy is applied. The strategy utilizes the actual reactive power flowing in the power system. The reactive current generated by the PV inverter actually compensates for the grid reactive current. This strategy is simple to actualize and is viable under all conditions particularly unbalanced disturbances.

2.3 Reactive Power Controller Operation

The PV inverter output currents are generated based on a three-phase reference or commanded current. The reference current will be used by the PV inverter controller to drive the PV inverter. The reference current comprises of active and reactive currents as well as unbalanced currents.

The reactive power controller works based on the idea that the reactive power created by the PV power plant relates to the actual reactive power in the power system. A current sensor on each phase is used on the grid side to generate the three-phase grid currents. From the sensor output currents, the control strategy aims at making a three-phase balanced active current ($I_{+\ active(a,b,c)}$). Then, the controller will naturally create reactive currents ($I_{+\ reactive(a,b,c)}$) as well as negative- and zero-sequence currents ($I_{-0\ (a,b,c)}$) for unbalanced system.

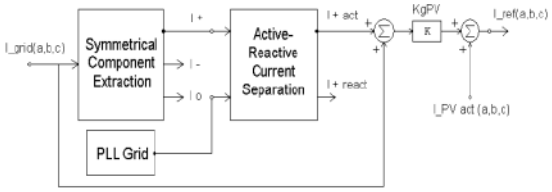

Fig. 2. A block diagram of a PV inverter controller for reactive power.

The block diagram of the PV inverter control strategy is described in Figure 2. From the output of grid current sensors, the controller segregates the three-phase grid currents into positive-, negative- and zero-sequence currents

using a symmetrical component extractor. Only the positive-sequence current is used. At that point, the three-phase positive-sequence current is divided into three-phase active and reactive positive-sequence currents by synchronizing to the grid voltages using a phase-locked loop (PLL) controller. The active currents are in-phase with the grid voltages, while the reactive currents are in quadrature with respect to the grid voltages. At last, the three-phase active positive-sequence current is subtracted from the measured grid currents to acquire a three-phase unbalanced reactive current ($I_{r(a,b,c)}$).

$$I_{r(a,b,c)} = I_{grid(a,b,c)} - I_{+\,active(a,b,c)} \quad (1)$$

or $$I_{r(a,b,c)} = I_{+\,reactive(a,b,c)} + I_{-0(a,b,c)} \quad (2)$$

However, for improving the voltage regulation at the PCC bus, the PV inverter will not support the full unbalanced reactive current ($I_{r(a,b,c)}$) for the entire power system. The inverter supplies just a small amount of the unbalanced reactive current according to the system impedance (multiplied by a gain, K_{gPV}).

The unbalanced reactive current is summed up with the PV active current ($I_{PV\ active}$) determined by solar irradiance. The result is the three-phase reference current.

$$I_{ref(a,b,c)} = I_{PV\ active(a,b,c)} + K_{gPV}\, I_{r(a,b,c)} \quad (3)$$

where K_{gPV} is a constant between 0 and 1.

If the PV inverter works very well, then the PV inverter output currents (I_{PV}) are the same as the reference currents.

$$I_{PV(a,b,c)} = I_{PV\ active(a,b,c)} + K_{gPV}(I_{+\,reactive(a,b,c)} + I_{-0(a,b,c)}) \quad (4)$$

2.4 Transformer Winding Connection

Standard winding connection of a three-phase power transformer is delta and star. Delta connection is more reliable than star connection. If one of the three windings fails, the delta configuration still works as open-delta connection with a three-phase balanced nominal voltage. On the other hand, the star connection can provide multiple voltages (phase-neutral and phase-phase voltages). The star configuration can supply single-phase and three-phase loads simultaneously.

The common primary and secondary windings of a three-phase transformer are star-delta and star-star [6][15]. The neutral of the star connection usually is grounded. In many applications, the star-delta configuration is popular because it is reliable and effective. Whereas, the star-star arrangement would be potentially unbalanced. In the star-delta winding connection, the star provides a neutral point, which is usually grounded for safety reasons to serve single-phase loads. The delta provides a better current balance for the grid. Compared to the star-star configuration, the star-delta configuration creates a voltage/current phase shift between primary and secondary sides. The delta connection also prevents the zero-sequence current flowing to the grid. For PV applications, there is Le-Blanc connection [14] for a special and complex configuration.

For grid-connected PV system, a step-up transformer is applied. The PV inverter is connected to the low voltage side of the transformer. For a delta and star configuration, the delta winding is usually connected to the high voltage grid, while the star winding is connected to the output terminal of the PV inverter.

3. Power System Under Study

A typical power system with PV installation under study is described in Figure 3. Bus 3 is a terminal of a main strong grid, which is represented by the Thevenin equivalent circuit (a voltage source with small impedance (Z_{34})). Small distribution system is connected to the bus 3. The typical PV installation is connected to the grid by means of long weak lines. The main interest is mostly on the power quality (voltage quality) at the point of connection of the PV inverter, since on the same bus (PCC), there may be regular and sensitive loads (e.g. electronic hardware).

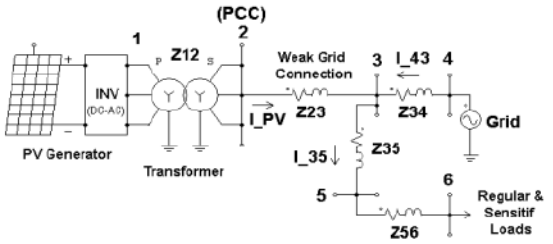

Fig. 3. A typical power system with PV installation.

From Figure 3, a high power PV generator is connected to the PCC (bus 2) through a power transformer (represented by impedance Z_{12}). The PV generator, which is a kind of distributed generation (DG), is usually situated far from the transmission line. Bus 2 is connected to bus 3 by means of a long weak line. It is considered a weak grid connection, which is ordinarily described by high impedance ($Z_{23} = Z_{weak}$). The short circuit ratio (SCR) at this point is smaller than 10. SCR is the ratio of PCC short circuit power to maximum apparent power of generator [13]. The system parameters under study are recorded in Table 1.

Table 1. System Parameter under Study.

MVA base	10MVA
KV base (L-L)	20kV
Z_{12}	7%
Z_{weak} (Z_{23})	50% (SCR ≈ 2)
Z_{34}	5%
Z_{35}	7%
Load (bus 5)	0.4pu, PF = 0.9 lag
K_{gPV}	0.1
Z_f	1%

From Figure 3, the voltage equation can be presented as follow:

$$V_2 = V_4 - I_{43}Z_{34} + I_{PV}Z_{23} \quad (5)$$

where $I_{43} + I_{PV} = I_{35}$ (6)

3.1 Transient Fault Conditions

The system in Figure 3 is examined under transient faults. When the system experiences a fault at bus 5, the high power PV installation is still connected to the electric network (fault ride-through) and attempts to support the voltage quality at the PCC. Only the main grid generates a large fault current. The PV generator as a current source will basically produces currents according to its control strategy.

During the fault, $I_{35} = I_f$. Since $I_f >> I_{PV}$, the current contribution from the PV inverter will not affect considerably the voltage at bus 3, so that $I_{43} \approx I_f$. For a solid ground fault, the bus-5 voltage is theoretically zero. While at bus 3 and bus 2, there is a severe voltage drop depending on the ratio Z_{35} to Z_{34}.

However, I_{PV} can be controlled such that the reactive currents produced by the PV inverter will improve the voltage at the PCC (bus 2). Assuming that X/R of the system impedance is high, and the PV unbalanced reactive current ($K_{gPV}\ I_{r(a,b,c)}$) supports the voltage regulation, K_{gPV} will be chosen as

$$K_{gPV} \approx \frac{Z_{34}}{Z_{23}} \quad (7)$$

So that according to equation (4) and (5) the voltage at bus 2 is corrected to

$$V_2 \approx V_4 - (I_{+\,reactive(a,b,c)} + I_{-0(a,b,c)})\, Z_{34} + \frac{Z_{34}}{Z_{23}} (I_{+\,reactive(a,b,c)} + I_{-0(a,b,c)})\, Z_{23} \quad (8)$$

Then the value of bus 2 voltage is close to bus 4 ($V_2 \approx V_4$). Thus, the disturbance effect of the fault is neutralized by the additional reactive power generated by the PV inverter and the ratio of the line impedance. The value of K_{gPV} is also applied to the normal condition.

4. Simulation Results

4.1 Star-star Winding Connection

a. Symmetrical faults

There is a three-phase to ground fault at bus 5 through Z_f in a brief timeframe (t = 0.7s – 1s). During the fault, the grid fault-current (I_f) ascends high (Figure 4 top). The fault will disturb the voltage of the neighboring buses. Without reactive power control, the three-phase voltage at PCC drops significantly to 0.732p.u (Figure 4 bottom).

The PV inverter with its controller senses the three-phase fault current (I_f) streaming in the grid and reacts rapidly by generating reactive currents to counteract the voltage dip at the PCC. A symmetrical fault creates only positive-sequence currents. Figure 5 (top) describes that the PV inverter output current is a summation of the active current (from solar irradiance, P_{PV} = 0.7pu) and the reactive current relative to the grid fault current. The PV inverter output current is conveyed to the grid through the star-star transformer with neutrals grounded. Figure 5 (bottom) exhibits that the system is stable and the PCC voltage is improved extremely well to a normal value (0.991p.u)) as projected by equation (8). The PCC voltage is balanced as well. Hence, the voltage quality is enhanced.

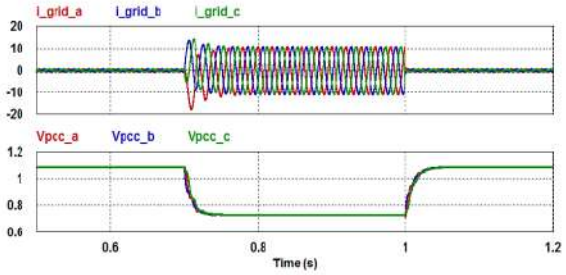

Fig. 4. A three-phase to ground fault (symmetrical fault): Grid fault currents (top), and voltages at PCC (bottom) without reactive power control.

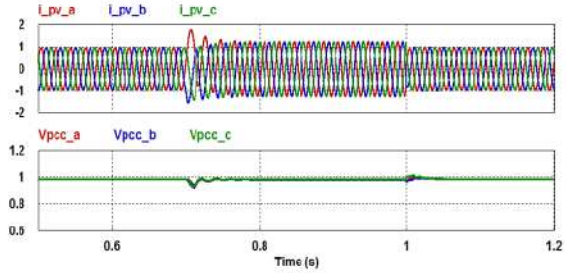

Fig. 5. A three-phase to ground fault (symmetrical fault): PV inverter output currents (top) and voltages at PCC (bottom) with reactive power control.

b. Unsymmetrical faults

The unsymmetrical faults observed in this paper are a line-to-line (LL) fault and a single-line to ground (SLG) fault. The faults through Z_f create unbalanced voltage and current. Thus, the PV inverter has to produce unbalanced reactive currents to compensate for the unbalanced faults. The active power from solar irradiance (P_{PV}) = 0.7pu.

b.1 Line-to-line (LL) fault

Figure 6 and 7 illustrate voltages at the PCC and grid currents when bus 5 experiences a LL fault between phase A and B (t = 0.7s – 1s). The grid currents are unbalanced. The phase-A and phase-B grid currents ascend high and stream to the faulty bus. Without reactive power control, phase A-B short circuit causes voltage drop to 0.755p.u at the phase A and to 0.898p.u at phase B, while the phase-C voltage stays around the normal value (1.07p.u).

The current sensors on the grid detect the fault currents. From the output of current sensors, a three-phase positive-sequence current is yielded by a symmetrical component extractor (Figure 8 top). The three-phase positive-sequence

current consists of three-phase active and reactive positive-sequence currents. As indicated by the control strategy, only the active positive-sequence current (Figure 8 bottom), which is in-phase with the fundamental grid voltage is developed for the following procedure.

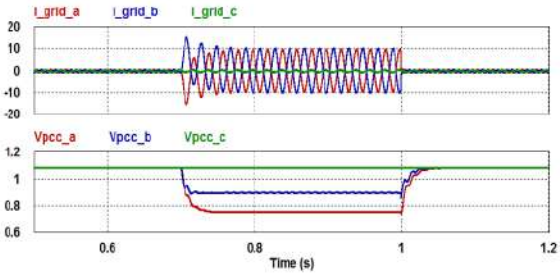

Fig. 6. A LL fault (unsymmetrical fault): Grid fault currents (top), and PCC voltages (bottom) without reactive power control.

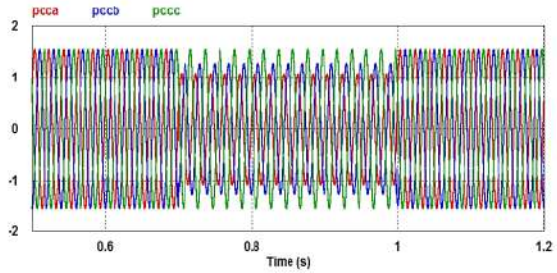

Fig. 7. A LL fault: the PCC voltage waveforms without reactive power control.

Furthermore, a three-phase unbalanced reactive current ($I_{r(a,b,c)}$) is naturally generated by comparing the three-phase active positive-sequence current to the three-phase grid current (Figure 9 top). Since the inverter delivers only a small amount of this current (Figure 9 bottom) to improve the PCC voltage quality, the unbalanced reactive current is normalized by a small gain (K_{gPV}).

At last, the three-phase reference current is obtained by adding the active current ($I_{PVactive} = 0.7$p.u) to the unbalanced reactive current as appeared in Figure 10 (top). The measure of active power is not affected by the disturbances. For dependent current source's gain equals one, the PV inverter output currents are the same as the reference currents. The PV inverter output currents are delivered to the grid through the star-star transformer with both neutrals grounded.

Figure 10 likewise shows that the system is stable, and the line voltage drop is corrected significantly. Figure 11 shows that the PCC voltages during disturbance are balanced. The voltage quality is improved.

b.2 Single line to ground (SLG) fault

Figure 12 illustrates the voltages at the PCC when bus 5 experiences a SLG fault at phase A (t = 0.7s – 1s). The phase-A grid current increases significantly flowing into the faulty bus. The phase-A grid current peak is about 10p.u (Figure 12 top). The grid currents are unbalanced as well. Without reactive power control, the phase-A voltage decreases to 0.732p.u, while other phases are a slightly greater than the nominal voltage (1.07p.u).

Using the same control strategy, the PV inverter generates unbalanced reactive currents similar to the grid fault currents with a small gain ($K_{gPV} = 0.1$). From Figure 13, the PV inverter produces total currents of unbalanced reactive currents and active currents ($I_{PVactive} = 0.7$p.u). Then, The PV inverter output current is delivered to the grid through the star-star transformer with neutrals grounded. The unbalanced voltage drop is compensated very well to be a three-phase balanced voltage (Figure 13 bottom). The system is stable and the voltage quality is upgraded.

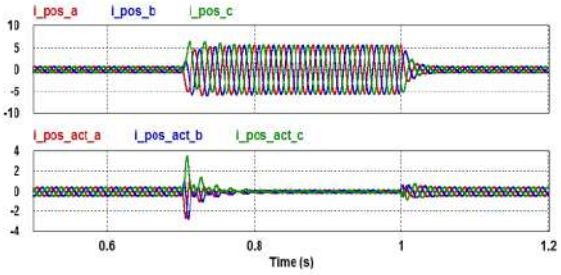

Fig. 8. A LL fault: A three-phase positive-sequence current (top), and a three-phase active positive-sequence currents (bottom).

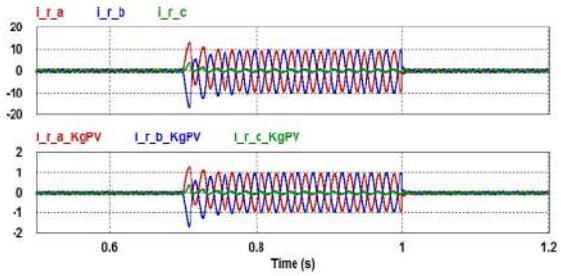

Fig. 9. A LL fault: A three-phase unbalanced reactive current (top), and a fraction of a three-phase unbalanced reactive current (bottom).

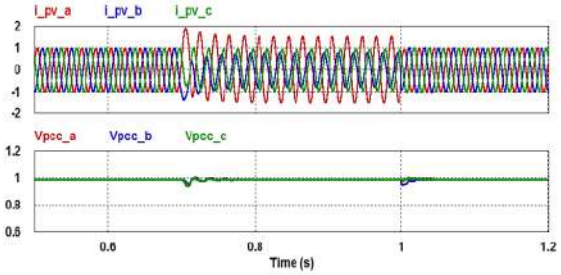

Fig. 10. A LL fault: PV inverter output currents (top), and voltages at PCC (bottom) with reactive power control.

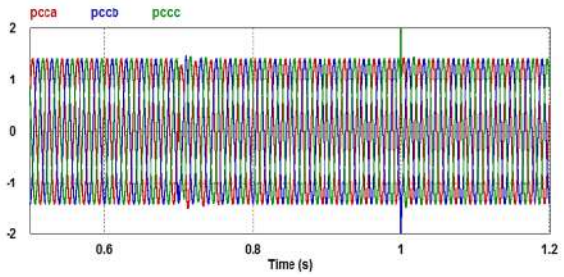

Fig. 11. A LL fault: The PCC voltage waveforms with reactive power control.

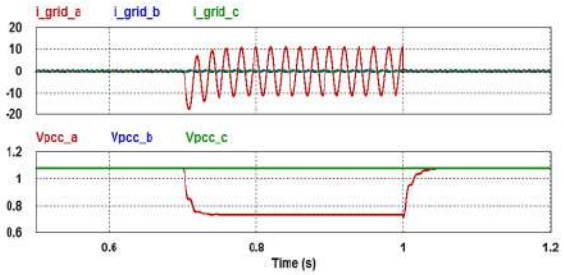

Fig. 12. A SLG fault (unsymmetrical fault): Grid fault currents (top), and voltages at PCC (bottom) without reactive power control.

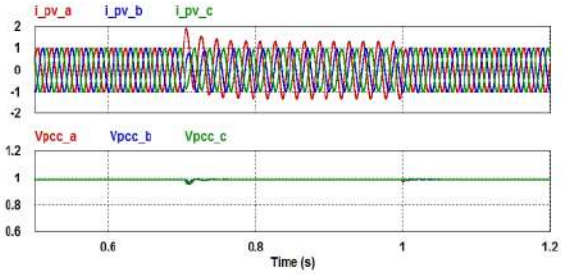

Fig. 13. A SLG fault: PV inverter output currents (top) and voltages at PCC (bottom) with reactive power control.

4.2 Star-delta Winding Connection

As mentioned above, the low voltage star winding is connected to the PV generator, while the high voltage delta winding is connected to the grid. For star-delta winding connection (e.g. YnD1), the winding ratio in per-unit system is 1:√3, and the phase shift is 30° (lagging). Therefore, the grid-connected PV system using a star-delta power transformer would create some problems if not corrected.

First, there is a voltage/current phase shift between the primary and the secondary sides of the transformer. The phase shift causes incorrect compensation. The PV inverter output current waveforms will be delayed 30° on the secondary side of the power transformer. The compensation currents do not match with the reference currents.

As a solution to this problem, the controller output is delayed with the same phase angle but in the opposite direction. As a result, the PV inverter output currents will be shifted 30° leading compared to the reference currents. After passing through the star-delta power transformer, the current waveforms will be in-phase with the reference current. This is done by means of a phase-shift controller or a delta-star signal transformer. For a YnD1 star-delta power transformer, the winding connection for the delta-star signal transformer is DYn11. The winding ratio in per-unit system is √3:1. The voltage/current is shifted 30° leading.

Secondly, the star-delta transformer will prevent the zero sequence current to flow. The zero-sequence component of the PV inverter output currents will circulate within the delta winding of the transformer. Therefore, star-delta winding connection inherently creates an open circuit for the zero-sequence currents to flow. If PV inverter output currents contain a zero-sequence component, then their waveforms will not be the same as the secondary-side current waveforms of the power transformer. A delta-star signal transformer and a phase shift controller cannot overcome this problem. Consequently, a fault that creates a zero-sequence current will get incorrect compensation.

To explain the control process in a star-delta power transformer, simulations are conducted for a three-phase to ground fault (a symmetrical fault) and a LL fault (an unsymmetrical fault) that both of them do not contain a zero-sequence current. Another simulation is a SLG fault (an unsymmetrical fault) that contains a zero-sequence current.

a. Symmetrical faults

Figure 14 shows (for phase-A) the controller output current after the reference current is shifted by 30° (leading) for a three-phase to ground fault. The PV inverter output current, which is the same as the controller output current is streaming through a star-delta power transformer. This current is shifted again by 30° but in the opposite direction (lagging). As a result, the secondary winding current is the same as the reference current. Figure 14 (bottom) shows that the three-phase secondary winding current is the same as the three-phase reference current.

Figure 15 reveals the good impact of a 30° phase shift controller on the PCC voltage for a three-phase to ground fault. The simulation results using a star-delta transformer and using a star-star transformer (Figure 5 and 15) are very similar. Without the phase shift strategy, the compensation results are incorrect. Figure 16 shows that the PCC voltages increase significantly under normal and fault conditions.

b. Unsymmetrical faults

b.1 Line-to-line (LL) fault

The control strategy for a LL fault is the same as for the three-phase to ground fault. Figure 17 shows that the three-phase secondary winding current is the same as the three-phase reference current for a LL fault when grid connection uses a star-delta transformer. During the fault, the PCC voltage unbalance are recovered to the normal value. The simulation results using a star-delta transformer and using a

star-star transformer (Figure 10 and 17) are very similar.

If the phase-shift strategy is not applied, the compensation is incorrect. Figure 18 demonstrates the voltages at the PCC for a LL fault without the 30° phase shift. As a result, the voltage quality decays.

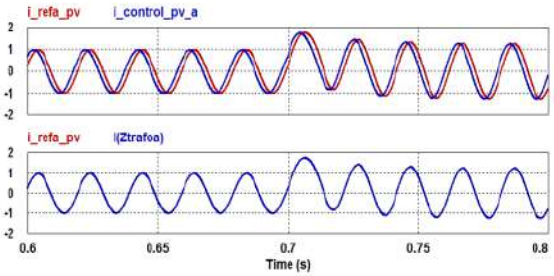

Fig. 14. A phase shift between the reference current and the controller output current (top), the secondary winding current is the same as the reference current (bottom) – phase A.

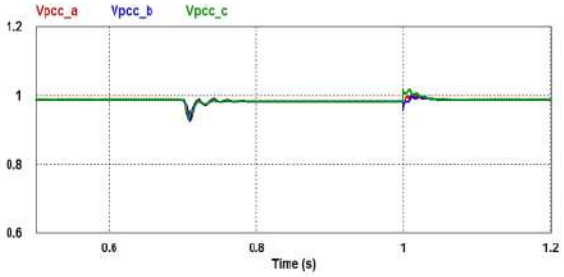

Fig. 15. PCC voltages for a three-phase to ground fault using a phase-shift strategy.

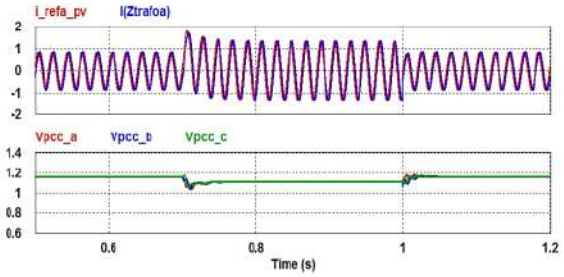

Fig. 16. Without a phase-shift strategy: The secondary winding current is different from the reference current (top), and PCC voltages (bottom) for a three-phase to ground fault.

b.2 Single line to ground (SLG) fault

Figure 19 depicts the PCC voltages under a SLG fault using a star-delta transformer with a phase-shift strategy. The simulation result during the fault is different from what is shown in Figure 13. In this fault, the zero sequence currents cease in the delta winding. The phase shift strategy cannot correct the disappearance of the zero-sequence current from the measured signal. During the fault, the transformer output currents are not the same as the reference currents (Figure 20). As a result, the PV inverter produce incorrect compensation. The voltage is not properly corrected.

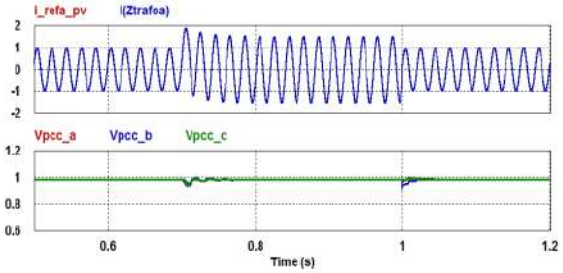

Fig. 17. With phase shift strategy: The secondary winding current is the same as the reference current (top), and the PCC voltages (bottom) for a LL fault.

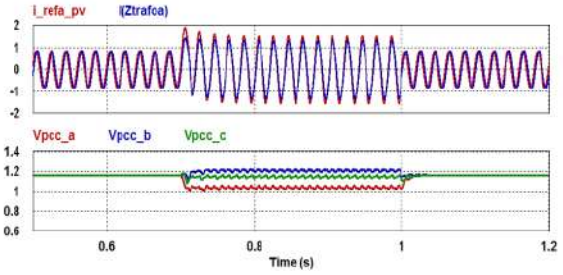

Fig. 18. Without phase shift strategy: The secondary winding current is different from the reference current (top), and the PCC is poor (bottom) for a LL fault.

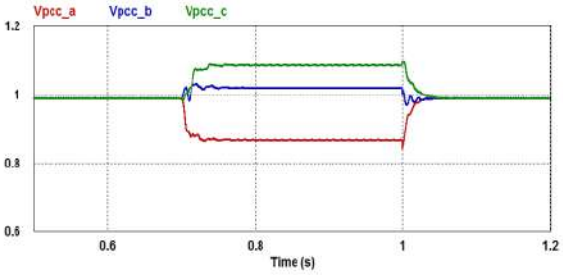

Fig. 19. Poor voltage quality at the PCC for a SLG fault using a star-delta transformer grid connection.

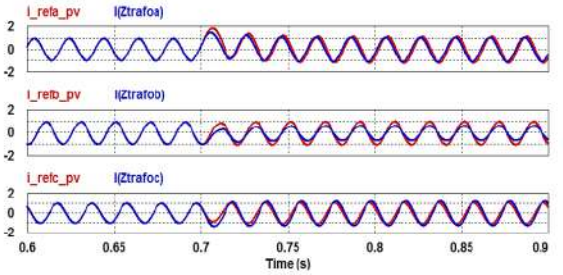

Fig. 20. Secondary winding currents are not the same as reference currents during a SLG fault.

5. Conclusions

This paper introduces the performance of transformer winding connections of a grid-connected PV. The high-power PV installation is connected to the weak grid by means of a three-phase power transformer. The PV source is modeled by an average model (e.g by a dependent current source). The PV inverter includes a reactive power controller to support voltage regulation of the system particularly under transient faults, which are both symmetrical and unsymmetrical faults. The control strategy is based on utilizing the grid currents to create a three-phase unbalanced reactive current with a small gain. The gain is determined by the system impedance.

Simulation results exhibit that the control strategy works very well if the transformer winding connection is star-star with both neutrals grounded. The power quality in terms of the voltage quality is improved. Under transient disturbances as well as normal condition, the PCC voltages are close to a nominal value (1p.u). The system is stable and voltage dips at the PCC due to the symmetrical and unsymmetrical faults are mitigated significantly.

If the transformer winding connection is changed to delta, a fault that creates a zero-sequence current cannot be compensated because it circulates within the delta winding. As a result, the voltage unbalanced cannot be fully corrected. For other faults such as a three-phase to ground fault and a line-to-line fault, the incorrect compensation due to star-delta winding phase shift can be handled by means of a phase-shift strategy. The PV inverter output currents will be shifted 30° leading compared to the reference currents. After passing through the star-delta power transformer, the current waveforms will be in-phase with the reference current. As a result, the voltage unbalanced is corrected.

Acknowledgements

This work was supported by the United States Department of State Bureau of Educational and Cultural Affairs and the National Renewable Energy Laboratory (NREL) under Fulbright Senior Research Program 2016.

References

[1] Arulkumar, K., Palanisamy, K., Vijayakumar, D., *Recent Advances and Control Techniques in Grid Connected PV System – A Review*, International Journal of Renewable Energy Research, Vol.6, No.3, 2016

[2] Eltawil, M.A., Zhao, Z., *Grid-Connected Photovoltaic Power Systems: Technical and Potential Problems—A Review*. Renewable and Sustainable Energy Reviews 14 (2010), p. 112–129

[3] Tumbelaka, H.H., L.J. Borle, and C.V. Nayar. *Analysis of a Series Inductance Implementation on a Three-phase Shunt Active Power Filter for Various Types of Non-linear Loads*. Australian Journal of Electrical and Electronics Engineering, Engineers Australia, Vol. 2, No. 3, 2005, p. 223-232.

[4] M. Calais et.al., *A Transformerless Five Level Cascaded Inverter Based Single Phase Photovoltaic System*, in IEEE proc. of 31st PESC, vol. 3, pp. 1173-1178, June 2000, Ireland.

[5] Rodriguez, J., Jih-Sheng Lai, Fang Zheng Peng, *Multilevel Inverters: A Survey of Topologies, Controls, and Applications*, IEEE Transactions on Industrial Electronics, Vol. 49, No. 4, pp. 724- 738, Aug 2002

[6] Alexey Kondrashov, Tobin Booth, *Distribution and Substation Transformers*, SolarPro Magazine, Issue 8.2, Mar/Apr '15

[7] L. Zhou, and Y. Chao, *The Research of Reactive Power Control Strategy For Grid-Connected Photovoltaics Plants*, in 2013 World Congress on Sustainable Technologies, pp. 12 – 17.

[8] H. Li, et. al., *Real and Reactive Power Control of A Three-Phase Single-Stage PV System and PV Voltage Stability*, in 2012 IEEE Power and Energy Society General Meeting, pp. 1 – 8.

[9] X. Su, et.al., *Optimal PV Inverter Reactive Power Control And Real Power Curtailment To Improve Performance Of Unbalanced Four-Wire LV Distribution Networks*, IEEE Transactions on Sustainable Energy, vol. 5, no. 3, 2014, pp. 967 – 977.

[10] P. Esslinger, and R. Witzmann, *Evaluation of Reactive Power Control Concepts For PV Inverter In Low-Voltage Grids*," in 2012 CIRED Workshop, paper 363.

[11] A. Camacho, et. al., *Flexible Voltage Support Control For Three-Phase Distributed Generation Inverters Under Grid Fault*, IEEE Transactions on Industrial Electronics, vol. 60, no. 4, 2013, pp. 1429 – 1441.

[12] Faa-Jen Lin, et. al., *Reactive Power Control of Three-Phase Grid-Connected PV System During Grid Faults Using Takagi-Sugeno-Kang Probabilistic Fuzzy Neural Network Control*, IEEE Transactions on Industrial Electronics, vol. 62, no. 9, 2015, pp. 5516 – 55528.

[13] N. P. W. Strachan, and D. Jovcic, *Stability of A Variable-Speed Permanent Magnet Wind Generator With Weak Ac Grids*, IEEE Transactions on Power Delivery, vol. 25, no. 4, 2010, pp. 2779 – 2788.

[14] V. Fernao Pires, et.al., *A Grid Connected Photovoltaic System with a Multilevel Inverter and a Le-Blanc Transformer*, International Journal of Renewable Energy Research, Vol.2, No.1, 2012

[15] M. Venkatesan, et.al., *A Fuzzy Logic Based Three phase Inverter with Single DC Source for Grid Connected PV System Employing Three Phase Transformer*, International Journal of Renewable Energy Research, Vol.5, No.3, 2015

[16] Luciano E.M. Calaca, et.al., *Multilevel Converter System for Photovoltaic Panels*, in 5th ICRERA, Nov 2016, pp. 913 – 918, Birmingham, UK.

[17] María A. Mantilla, et.al., *Control of active and reactive powers in three phase inverters for grid tied photovoltaic systems under unbalanced voltages*, in 3rd ICRERA, Oct 2014, pp 583 – 588, Milwaukee, USA.

The effect of transformer Winding

ORIGINALITY REPORT

7%	2%	5%	3%
SIMILARITY INDEX	INTERNET SOURCES	PUBLICATIONS	STUDENT PAPERS

PRIMARY SOURCES

1	Submitted to Technological Institute of the Philippines Student Paper	2%
2	dergipark.ulakbim.gov.tr Internet Source	1%
3	"Innovation in Electrical Power Engineering, Communication, and Computing Technology", Springer Science and Business Media LLC, 2020 Publication	1%
4	"Artificial Intelligence in Renewable Energetic Systems", Springer Science and Business Media LLC, 2018 Publication	1%
5	www.semanticscholar.org Internet Source	1%
6	Chaouki Ghenai, Maamar Bettayeb. "Modelling and performance analysis of a stand-alone hybrid solar PV/Fuel Cell/Diesel Generator power system for university building", Energy,	1%

2019
Publication

7	Tiago Davi Curi Busarello, Ali Mortezaei, Adriano Peres, Marcelo Godoy Simoes. "Application of the Conservative Power Theory Current Decomposition in a Load Power-Sharing Strategy Among Distributed Energy Resources", IEEE Transactions on Industry Applications, 2018 Publication	1%
8	"Proceedings of International Conference on Artificial Intelligence, Smart Grid and Smart City Applications", Springer Science and Business Media LLC, 2020 Publication	1%

Exclude quotes	On	Exclude matches	< 1%
Exclude bibliography	On		